



Oscillations of Water Levels in Vertical Semi-Immersed Tubes: Analytical Solutions and Experimental Verification

H. E. Schulz^{1,2†} and D. Z. Zhu²

¹ School of Engineering at São Carlos, University of São Paulo, São Carlos, SP, ZIP 13566-590, Brazil

² Dept. of Civil and Environmental Engineering, University of Alberta, Edmonton, AB, T6G 2W2, Canada

†Corresponding Author Email: heschulz@sc.usp.br

(Received February 2, 2017; accepted July 9, 2017)

ABSTRACT

Experimental results for water level oscillations in vertical tubes, together with a theoretical solution for the flow in such tubes considering local and distributed energy losses, are presented and compared. The experimental data were obtained in small scale experiments, allowing adequately controlling the oscillations. The governing equation for the oscillations was obtained by applying the conservation laws of mass, momentum and energy for fluids. It is a second order nonlinear differential equation which was reduced to a first order differential Bernoulli equation. The obtained solution is composed by two different equations, one for the upwards motion and the other for the downwards motion, which together reproduce the oscillatory damped behavior of such flows. Numerical solutions of the differential equation were also checked. The experimental data and the theoretical and numerical results showed a good agreement between measured and calculated values of velocity and surface level for the first periods of oscillation.

Keywords: Water level fluctuations; Damped fluctuations; Oscillation suppressing devices; Applied nonlinear differential equations.

NOMENCLATURE

A	area	T	period of oscillation
D	diameter of the tube	V	nondimensional water velocity
F	force	V_R	dimensional water velocity
F_L	resistive force	V_{ol}	volume
f	friction factor	y	nondimensional water level
g	acceleration of gravity		
h	dimensional water level	θ_1	coefficient
H_R	reference height or equilibrium position	θ_2	coefficient
K	local energy loss coefficient	θ_3	coefficient
L	length of volume of water in a tube	ρ	water density
N	natural number $N=2\theta_3$	τ	nondimensional time
t	dimensional time		

1. INTRODUCTION

The possibility to predict the oscillations of water levels and velocities in water pipes is relevant for several applications in engineering. The use of oscillation suppressing devices in supply pipes for power generation turbines is perhaps the most classical example. Surge tanks and air chambers with or without orifices are among such devices,

which may be adapted to vertical pipes, pointing to the convenience of studying with more details the flows in vertical pipes. As additional example, the somewhat uncontrolled growing of cities in the last century introduced some problems related to the drainage system of such “oversized” human centers. (Lou *et al.*, 2008, for example). Vertical pipes that mainly conduct the excess of water from the surface to the horizontal buried pipelines may be subjected

to situations not predicted in the original design. The drainage systems may be flooded, generating geysers and level oscillations in the vertical pipes, which may propagate along the drainage system inducing damages. Considering the underground characteristic of such systems, it may be difficult and costly to repair damages.

A sketch of the geometrical disposition of vertical tubes in drainage systems is shown in Fig. 1. The arrangements of the horizontal system of pipelines add particularities that must be considered in each design situation. (Politano *et al.*, 2005, for example)

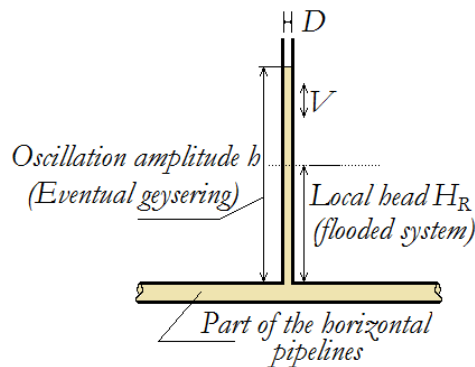


Fig. 1. Sketch of the geometry of a vertical tube and horizontal pipelines in drainage systems. D is the diameter and V is the velocity of the flow.

Predicting oscillations in vertical pipes naturally leads to comparisons between “free oscillation” and “damped oscillation” conditions, being the “damped oscillation” cases imposed by installed devices. In this sense, numerical procedures applied to proper governing equations are of practical use, giving quick support to professionals dealing with this theme. Numerical calculations impose calibration procedures, which also exposes the need of proper theoretical predictions or conveniently conducted experiments. Both controlled experimental data for isolated vertical columns and theoretical predictions for such flows are still somewhat rare in the literature, being convenient to spend some effort to provide an adequate bank of data, together with theoretical solutions for basic flows. One example of theoretical solutions is the study of Lorenceau *et al.* (2002), in which local losses are taken into account to obtain the solution. The distributed losses are considered only numerically using the first power of the velocity (laminar condition), and in discussions about large viscous effects related to threshold viscosity values that allow the appearance of oscillations (limiting viscosity values that totally damp oscillating movements). Considering smaller dimensions (diameters) of the tube, results and theoretical predictions involving capillarity are found in Zhmud *et al.* (2000), Quéré and Raphaël (1999), and Lorenceau *et al.* (2002), for example.

Flows in vertical pipes involve arduous themes like bubble transport (Benattalah *et al.* 2011), settling instability (Weidman *et al.*, 2012) or solids transport in gas flows (El-Behery *et al.*, 2017), for

example. These are beyond the scope of the present study.

This study furnishes a nondimensional theoretical solution for the velocity of the flow in vertical tubes, obtained for a governing equation with local and distributed energy losses, considering turbulent condition, that is, losses are proportional to the square of the mean velocity. Further, experimental data of oscillating flows in vertical tubes are furnished to consider the main characteristics of the observed flow.

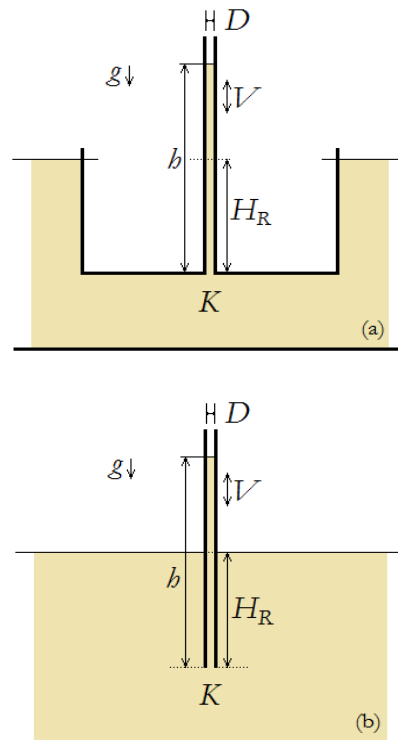


Fig. 2. a) Oscillating column with pipe out of the water and main variables of Fig. 1; b) Oscillating column with semi-immersed pipe and the corresponding variables of case (a).

2. EXPERIMENTAL DEVICES

In this study the oscillations of the water level were observed in vertical pipes with constant diameters, subjected to local energy losses (at the pipe entrance) and distributed losses (friction losses along the tube).

Two arrangements were initially considered for observing oscillations without the need to quantify particularities of horizontal pipelines: i) pipe out of the water (Fig. 2a), and ii) semi-immersed pipe (Fig. 2b). The arrangement of Fig. 2a is perhaps easier to relate to surge tanks and vertical tubes in drainage systems like shown in Fig. 1. But it works similar to the semi-immersed tube of Fig. 2b, being the last much easier to build in a laboratory. Eventual distinctions exist for the inlet/outlet loss coefficient K , because it depends on the local

geometry, but they are not relevant in the present study. The arrangement of Fig. 2b was used here, being simple and elegant to obtain oscillation results for isolated vertical columns. It is similar to that used by *Lorenceanu et al. (2002)*.

2.1 Laboratory Setups

Two setups were built to obtain results for the position and the velocity of the oscillating surface under controlled situations: a small scale setup, with the vertical tube having a diameter of 0.62 cm, and a large scale setup, with the vertical tube having a diameter of 2.54 cm, shown here in Fig. 3. Both setups had similar constructive arrangements. The different scales allowed obtaining different sets of data to compare with the theoretical predictions.

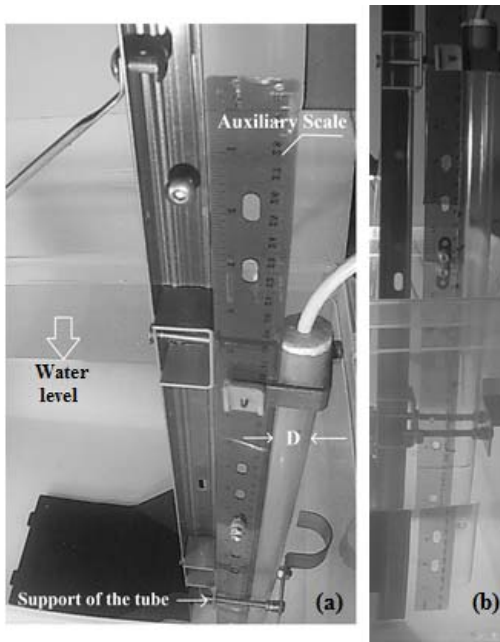


Fig. 3. Large scale oscillating column following Fig. 2b, with diameter $D=2.54\text{cm}$.; a) Detail of the upper part of the setup; b) Lateral view.

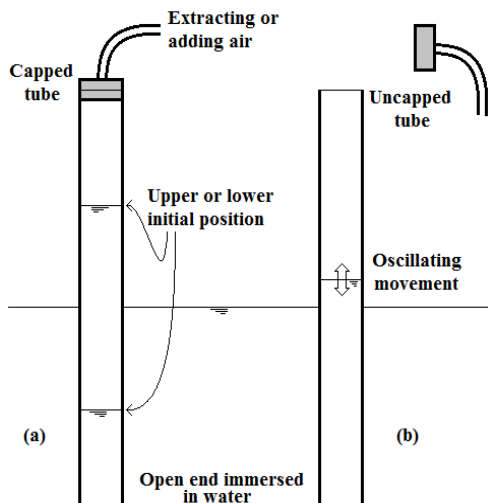


Fig. 4. Adjusting the initial condition using a cap linked to a hose.

Figure 3a shows the vertical tube capped and linked to a hose. The cap and hose allowed setting the initial water level to start the oscillations, as shown in Figs. 4a and 4b. Air was added to or extracted from the vertical tube through the hose, which was then closed imposing the initial condition. To run the experiment, the cap was removed and the water began to oscillate.

2.2 Measured Values

Tables 1 to 4 present experimental data obtained by filming runs of oscillating flows in the two described setups. The data of time, level and velocity were obtained from frame by frame analysis of the recorded films. The frames were individualized using the ‘instantaneous’ tool of the Windows ® Life Movie Maker software. The level of the water was measured from each frame using a digital image program (Paint ® of the Windows ® operational system). The record speed (in fps) allowed determining the mean velocity of the surface between two sequent water level registers.

The data of the first two tables were recorded with a digital camera at a speed of 30 fps. The third table was obtained with a second camera at 120 fps. In this case, the two first periods of oscillation were computed for 120 fps, the third period for 60 fps, and the subsequent data for 40 fps. Small amplitudes allow using the usual filming velocities (30 fps) or the lower range of 40 to 60 fps, as done here. But larger amplitudes need higher speeds. The fourth table presents data for damped oscillations. Only the first period of oscillation is furnished, and was obtained with the camera at 60 fps.

3. GOVERNING EQUATION

Considering the variables shown in Fig. 2b, the governing equation for the position of the water level along time in the vertical pipe was obtained. The integral equations for mass and momentum conservation were applied in the control volume given by the internal volume of the tube with length h for homogeneous variables at the cross sections furnishing, respectively:

$$\rho A \frac{dh}{dt} - \rho AV_R = 0 \quad (1)$$

$$F = \rho AV_R \frac{dh}{dt} + \rho Ah \frac{dV_R}{dt} - \rho AV_R^2 \quad (2)$$

The variables are defined in the NOMENCLATURE table. The force F is calculated considering the hydraulic head H_R , the weight of the column, and the resistive force during the movement, expressed as F_L . Mathematically, for upwards movement:

$$F = \rho A g H_R - \rho A g h - F_L \quad (3)$$

The resistive force is evaluated through the pressure difference caused by energy losses using the Darcy-Weisbach equation for distributed losses, and adequate coefficients for local losses. The result is:

$$F = \rho A g \left[H_R - h - \left(\frac{fhV_R^2}{2gD} + \sum_i \frac{K_i V_R^2}{2g} \right) \right] \quad (4)$$

Eqs. (1), (2), and (4) allow replacing Eqs. (1) and (2), respectively, by:

$$\frac{dh}{dt} = V_R \quad (5)$$

$$h \frac{dV_R}{dt} = g(H_R - h) - \frac{fh}{D} \frac{V_R^2}{2} - \sum_i \frac{K_i V_R^2}{2} \quad (6)$$

Equation (6) can also be derived from the integral energy equation, together with the Darcy-Weisbach equation and local loss coefficients. Inserting Eq. (5) into Eq. (6) it follows that:

$$h \frac{d^2h}{dt^2} = g(H_R - h) - \frac{fh}{2D} \left(\frac{dh}{dt} \right)^2 - \sum_i \frac{K_i}{2} \left(\frac{dh}{dt} \right)^2 \quad (7)$$

Equation (7) was converted into a nondimensional form by using

$$\theta_1 = \pm 1, \theta_2 = \frac{fH_R}{2D}, \theta_3 = \sum_i \frac{K_i}{2}, y = \frac{h}{H_R}, \tau = \sqrt{\frac{g}{H_R}} t \quad (8)$$

The final nondimensional governing equation of the water level along the time in the vertical pipe is:

$$\frac{d^2y}{d\tau^2} = \left(\frac{1}{y} - 1 \right) + \theta_1 \left(\theta_2 + \frac{\theta_3}{y} \right) \left(\frac{dy}{d\tau} \right)^2 \quad (9)$$

The signs + and - in θ_1 mean downwards and upwards motions, respectively. It is convenient to mention that θ_3 , which computes local losses (and momentum flows through the control surface), may be different for upwards and downwards motions. This is evidenced in studies for capillary tubes, as for example Masoodi *et al.* (2014), and Lorenceau *et al.* (2002). y and τ of Eq. (9) are nondimensional variables for level and time that allow better comparison between results of different geometries. It is a second order nonlinear equation, in principle having no general rules for its integration. As inferred from Eqs. (8), θ_2 and θ_3 depend on the flow conditions (laminar or turbulent) and on the geometrical aspects of the tubes, like the form of the inlet/outlet and the roughness of the inner surface. These aspects may be considered in numerical procedures by inserting empirical information, like the Churchill equation for friction factors (Churchill, 1977). But for testing the convergence of numerical schemes to theoretical results, constant values of θ_2 and θ_3 can be used to obtain the theoretical solutions, procedure followed here. Lorenceau *et al.* (2002, p.1989) presented an equation similar to Eq. (9), but with the parcel involving θ_2 (distributed losses) multiplied by the first power of the velocity, and not by the second power like in the present study. Eq. (9) was here converted into a first order Bernoulli equation. In

addition to the definitions of Eqs. (8), the nondimensional velocity is given by:

$$V = V_R / \sqrt{gH_R} \quad (10)$$

The variables V , y and τ were used into Eq. (6). After simplifying constants, it is obtained that:

$$\frac{dV}{d\tau} = \left(\frac{1}{y} - 1 \right) + \theta_1 \left(\theta_2 + \frac{\theta_3}{y} \right) V^2 \quad (11)$$

From Eqs. (9) and (11) it is seen that $dy/d\tau = V$. By defining:

$$W = V^{-1} \quad (12)$$

It follows that:

$$W dy = d\tau \quad (13)$$

Equations (11), (12), and (13) produce

$$\frac{dW}{dy} = \left(\frac{1}{y} - 1 \right) W^3 - \theta_1 \left(\theta_2 + \frac{\theta_3}{y} \right) W \quad (14)$$

This is an integrable first order Bernoulli equation.

3.1 General Solution

Solutions for V were obtained for the upwards motion ($\theta_1=-1$) and the other for the downwards motion ($\theta_1=+1$), in the form:

$$V_N^{Up} = \sqrt{\frac{\sum_{i=0}^{N-1} \frac{(N-1)! (-1)^{N-1+i} y^i}{i! (2\theta_2)^{N-i}} - \sum_{i=0}^N \frac{N! (-1)^{N+i} y^i}{i! (2\theta_2)^{N+1-i}} + C e^{-2\theta_2 y}}{(y^N)/2}} \quad (15)$$

$$V_N^{Down} = \left\{ -2 y^N \left[\sum_{i=1}^N \frac{(i-1)! (-2\theta_2)^{N-i}}{N! y^i} - \sum_{i=1}^{N-1} \frac{(i-1)! (-2\theta_2)^{N-1-i}}{(N-1)! y^i} \right] + 2 e^{2\theta_2 y} y^N \left[\frac{(-2\theta_2)^N}{N!} - \frac{(-2\theta_2)^{N-1}}{(N-1)!} \right] \left[\ln y + \sum_{j=1}^{\infty} \frac{(-2\theta_2 y)^j}{j \cdot j!} \right] + C e^{2\theta_2 y} y^N \right\}^{\frac{1}{2}} \quad (16)$$

The upper indexes *Up/Down* indicate the direction of the motion of each solution. C represents the integration constant. $N=2\theta_3$ is a natural number ($N=1, 2, 3, \dots$). When using the theoretical solution for predictions, the “physically real” θ_3 must be adjusted to the closest adequate N . Eq. (16) shows that the downwards motion involves an infinite sum

of powers of y . The nondimensional procedures followed here implied in y close to one (1.0) for the calculated examples, so that the infinite series converged using 13 parcels (that is, $j=13$). The number of parcels depends on y .

Tables 1 and 2 Data for $D=0.62$ cm, 30 fps

Table 1 H_R (cm)=7.50			Table 2 H_R (cm)=5.80		
t s	h cm	V_R cm/s	t s	H cm	V_R cm/s
0.033	0.82	9.55	0.033	0.72	6.04
0.066	2.00	35.5	0.066	2.45	52.0
0.100	4.00	60.0	0.100	4.43	59.2
0.133	5.91	57.3	0.133	5.64	36.3
0.167	7.59	50.5	0.167	6.76	33.8
0.200	8.55	28.6	0.200	7.57	24.2
0.233	9.64	32.7	0.233	8.25	20.5
0.267	10.41	23.2	0.267	8.45	6.04
0.300	10.77	10.9	0.300	8.29	-4.83
0.333	10.82	1.36	0.333	8.01	-8.46
0.367	10.64	-5.45	0.367	7.42	-16.9
0.400	10.23	-12.3	0.400	6.72	-21.8
0.433	9.36	-25.9	0.433	5.80	-27.8
0.467	8.50	-25.9	0.467	5.27	-15.7
0.500	7.73	-23.2	0.500	4.75	-15.7
0.533	6.73	-30.0	0.533	4.59	-4.83
0.567	6.00	-21.8	0.567	4.71	3.63
0.600	5.77	-6.82	0.600	5.11	12.1
0.633	5.82	1.36	0.633	5.68	16.9
0.667	6.14	9.55	0.667	6.00	9.67
0.700	6.45	9.55	0.700	6.40	12.1
0.733	7.00	16.4	0.733	6.64	7.25
0.767	7.64	19.1	0.767	6.64	0.00
0.800	8.05	12.3	0.800	6.72	2.41
0.833	8.32	8.18	0.833	6.48	-7.25
0.867	8.50	5.45	0.867	6.28	-6.04
0.900	8.36	-4.09	0.900	6.08	-6.04
0.933	8.23	-4.09	0.933	5.76	-9.67
0.967	8.05	-5.45	0.967	5.68	-2.42
1.000	7.73	-9.55	1.000	5.55	-3.63
1.033	7.36	-10.9	1.033	5.60	1.21
1.067	7.14	-6.82	1.067	5.63	1.21
1.100	7.09	-1.36			
1.133	7.09	0.00			

3.2 Solution for $N=2$

To perform calculations and compare the theoretical solution with numerical results, the lower natural values $N=2$ and $\theta_2=1$ were used. They generate the typical oscillating behavior through equations that

are sufficiently short for a more immediate analysis. The same value of θ_3 was used for the upwards and downwards motions, producing Eqs. (17) and (18):

$$V_2^{Up} = \sqrt{-\left(1 - \frac{1}{y}\right)^2 + Cy^{-2}e^{-2y}} \tag{17}$$

$$V_2^{Down} = \sqrt{e^{2y}y^2 \left[-\frac{e^{-2y}}{y^2} + 4\frac{e^{-2y}}{y} + 8\ln y + 8\sum_{i=1}^{\infty} \frac{(-2y)^i}{i \cdot i!} + C \right]} \tag{18}$$

For the calculations, the constant of integration C must be adjusted for the initial condition of every upwards and downwards half period. The initial velocity in each half period is $V=0$ (rest). The initial value of y for the problem is the observed value (known). The start y value of each subsequent half period is the last y value of the previous half period (also known). The values of C are then determined.

3.3 Numerical Calculations

As mentioned, theoretical solutions may be used during calibration procedures as a way of checking the quality of numerical calculations. They also allow observing how different control parameters of the governing equation (for example, the parameters that quantify energy losses) are linked to observable parameters (water level, for example). In this case, Eqs. (15) and (16) show that the distributed losses (θ_2) are linked to exponential terms, while the local losses (θ_3 or $N/2$) determine the limiting power value of y in the sums of powers of y (water level).

A numerical procedure was necessary to show that the theoretical solutions furnished here correspond to proper solutions of the original problem given by the second order nonlinear Eq. (9). An expeditious explicit “one-forward-step” procedure was adopted to perform this checking. The discrete quantities given by following Eqs. (19) and (20) are obtained immediately from Eq. (9):

$$V = \frac{dy}{d\tau}, \quad \text{thus} \quad y_{i+1} = y_i + V_i \Delta\tau \tag{19}$$

$$\frac{dV}{d\tau} = \left(\frac{1}{y} - 1\right) + \theta_1 \left(\theta_2 + \frac{\theta_3}{y}\right) V^2, \quad \text{thus}$$

$$V_{i+1} = V_i + \left[\left(\frac{1}{y_i} - 1\right) + \theta_1 \left(\theta_2 + \frac{\theta_3}{y_i}\right) V_i^2 \right] \Delta\tau \tag{20}$$

The iterative one-forward-step procedure is resumed as:

- 1 To furnish the control parameters θ_1 , θ_2 , and θ_3 , and the time increment $\Delta\tau$.
- 2 To furnish the initial conditions y_i , V_i , $i=0$.
- 3 To calculate V_{i+1} using Eq. (20).
- 4 To calculate y_{i+1} using Eq. (19).

- 5 To repeat steps 3 and 4 until attaining the desired final condition.

4. RESULTS AND DISCUSSION

4.1 Theoretical and Numerical Results

Equations (17) and (18) form a set for the up/down motion of the water column when using $\theta_2=1$ and $\theta_3=1$ (or $N=2$). Fig. 5 shows the evolution of the obtained functions in the phase plot (y, V) . The attractor structure converging to the fixed point $(1,0)$ is expected, considering that it reflects a damped oscillatory movement. Similar plots may be found, for example, in Weidman and Kllakhandler (2014), for capped liquid-air columns.

Each part of the solution itself, that is, Eq. (17) *Up* and Eq. (18) *Down*, is not a periodic movement in the (y, V) plane. Only both solutions together confer a cyclic character to the predicted motion. Note that also the real movement is not the projection of a cyclic movement continuous in time. It is in fact composed by a succession of inverse motions intercalated by moments of rest, that is, a sequence of juxtaposed “pieces” of movement of the water column. Despite this correspondence between real motion and theoretical solutions, this “piecewise aspect” of the solution may induce doubts about the complementarity of Eqs. (17) and (18). The numerical result was thus necessary to show that, although represented by two distinct functions, the two equations do correspond to the solution of the original governing equation, tested for $\theta_2=1$ and $\theta_3=1$ (or $N=2$). Fig. 5 shows that the agreement between numerical results and analytical solutions is very good, confirming that Eqs. (15) and (16) may be used as tools for subsequent studies in this field. For example, more complex numerical codes may be tested with this simpler situation, for which the theoretical solution is now furnished.

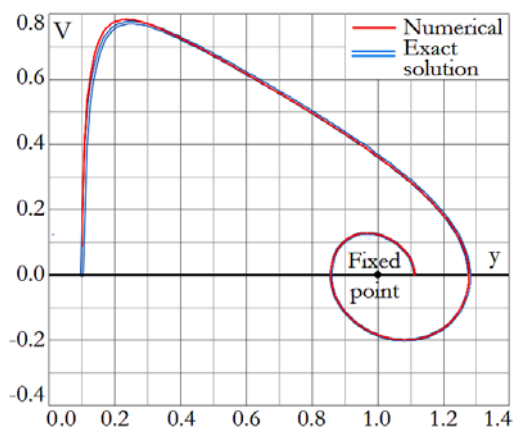


Fig. 5. Good agreement of numerical and exact results show that the theoretical equations can be used to calibrate numerical codes for simpler situations. $\theta_2=1.0$, $\theta_3=1.0$, $\Delta\tau=0.01$.

4.2 Results of the Small Setup

Figure 6 shows the measured data of Tables 1 and 2

plotted together with numerical results in the (y, V) plane. The data are for free oscillations (not damped) in the tube with diameter of 0.62 cm. H_R was fixed at 5.8 cm and 7.5 cm. The normalized immersion lengths H_R/D thus were 9.4 and 12.1, respectively. The experimental velocity values were obtained from the difference between two successive measured heights divided by the time interval between the measurements, characterizing the mean velocity for this time interval. It was plotted against the mean height obtained from the two limiting heights of each time interval. The use of mean values implied in a shift in the time scale of Fig. 7, which presents the evolution of the nondimensional mean water level (considering the time interval) in the vertical tube plotted against the nondimensional time. Figs. 6 and 7 used the same data. The results show that numerical calculations and experimental values follow similar trends in these initial periods of oscillation.

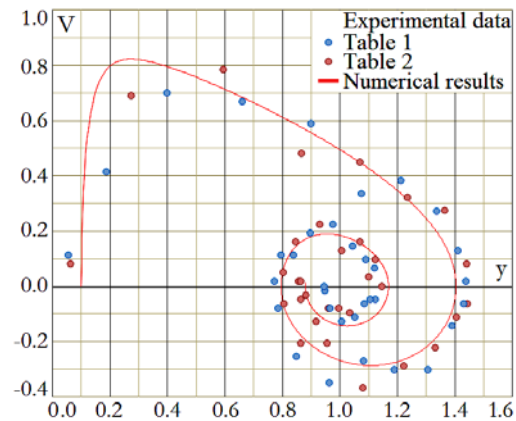


Fig. 6. Experimental data of Tables 1 and 2 and numerical results of Eq. (9) for $\theta_2=0.3$, $\theta_3=1.0$, $\Delta\tau=0.01$.

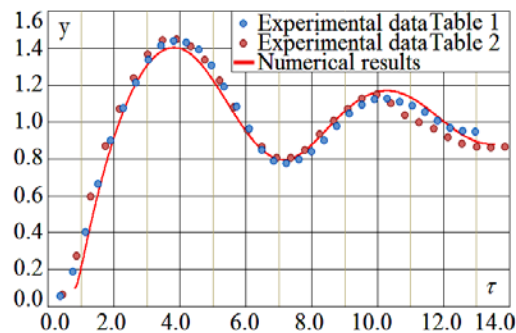


Fig. 7. Time evolution of the nondimensional height for the same conditions of Fig. 6.

As mentioned, the data of Tables 1 and 2 were obtained in the small setup, corresponding mostly to the lower range of the Reynolds number (highest Reynolds number of 3,720), being also subjected to capillary effects. However, despite these conditions, data and calculations agreed well for the first periods using constant coefficients. The coefficients were fixed in $\theta_2=0.3$, $\theta_3=1.0$, for both runs. Note that the usual friction factors are valid for

Table 3 Data for $D=2.54$ cm. Nondimensional variables, 120, 60 and 40 fps. τ given by Eq. (8)

τ	b/H_R mean	V mean												
0.183	0.042	0.000	4.277	1.463	-0.191	8.370	1.023	0.268	12.464	0.867	-0.191	19.368	0.867	-0.076
0.244	0.047	0.076	4.338	1.449	-0.229	8.431	1.042	0.306	12.525	0.855	-0.191	19.490	0.857	-0.076
0.305	0.056	0.153	4.399	1.428	-0.344	8.493	1.061	0.306	12.586	0.843	-0.191	19.612	0.853	-0.038
0.367	0.065	0.153	4.460	1.414	-0.229	8.554	1.079	0.306	12.647	0.832	-0.191	19.734	0.853	0.000
0.428	0.084	0.306	4.521	1.395	-0.306	8.615	1.096	0.268	12.708	0.825	-0.115	19.857	0.855	0.019
0.489	0.107	0.382	4.582	1.374	-0.344	8.676	1.112	0.268	12.769	0.815	-0.153	19.979	0.860	0.038
0.550	0.164	0.918	4.643	1.357	-0.268	8.737	1.126	0.229	12.830	0.806	-0.153	20.101	0.862	0.019
0.611	0.196	0.535	4.704	1.336	-0.344	8.798	1.143	0.268	12.892	0.797	-0.153	20.223	0.874	0.096
0.672	0.229	0.535	4.766	1.308	-0.459	8.859	1.157	0.229	12.953	0.792	-0.076	20.406	0.893	0.102
0.733	0.278	0.803	4.827	1.283	-0.421	8.920	1.173	0.268	13.014	0.787	-0.076	20.590	0.911	0.102
0.794	0.343	1.071	4.888	1.262	-0.344	8.981	1.185	0.191	13.075	0.783	-0.076	20.773	0.930	0.102
0.855	0.400	0.918	4.949	1.238	-0.382	9.042	1.194	0.153	13.136	0.783	0.000	20.956	0.951	0.115
0.916	0.449	0.803	5.010	1.215	-0.382	9.103	1.206	0.191	13.197	0.783	0.000	21.140	0.972	0.115
0.978	0.498	0.803	5.071	1.189	-0.421	9.165	1.215	0.153	13.258	0.780	-0.038	21.323	0.991	0.102
1.039	0.542	0.727	5.132	1.166	-0.382	9.226	1.222	0.115	13.319	0.780	0.000	21.506	1.012	0.115
1.100	0.584	0.688	5.193	1.140	-0.421	9.287	1.229	0.115	13.380	0.783	0.038	21.690	1.030	0.102
1.161	0.629	0.727	5.254	1.114	-0.421	9.348	1.238	0.153	13.441	0.783	0.000	21.873	1.054	0.127
1.222	0.668	0.650	5.315	1.091	-0.382	9.409	1.243	0.076	13.503	0.785	0.038	22.056	1.075	0.115
1.283	0.710	0.688	5.377	1.063	-0.459	9.470	1.252	0.153	13.564	0.787	0.038	22.239	1.093	0.102
1.344	0.757	0.765	5.438	1.030	-0.535	9.531	1.257	0.076	13.625	0.792	0.076	22.423	1.105	0.064
1.405	0.804	0.765	5.499	0.995	-0.574	9.592	1.262	0.076	13.686	0.799	0.115	22.606	1.117	0.064
1.466	0.853	0.803	5.560	0.965	-0.497	9.653	1.269	0.115	13.747	0.804	0.076	22.789	1.124	0.038
1.527	0.893	0.650	5.621	0.939	-0.421	9.714	1.276	0.115	13.809	0.818	0.115	22.973	1.124	0.000
1.589	0.928	0.574	5.682	0.907	-0.535	9.776	1.280	0.076	13.991	0.836	0.153	23.156	1.124	0.000
1.650	0.958	0.497	5.743	0.883	-0.382	9.837	1.283	0.038	14.113	0.860	0.191	23.339	1.124	0.000
1.711	0.995	0.612	5.804	0.857	-0.421	9.898	1.283	0.000	14.236	0.886	0.210	23.522	1.119	-0.025
1.772	1.035	0.650	5.865	0.829	-0.459	9.959	1.283	0.000	14.358	0.909	0.191	23.706	1.110	-0.051
1.833	1.075	0.650	5.926	0.801	-0.459	10.020	1.283	0.000	14.480	0.932	0.191	23.889	1.100	-0.051
1.894	1.112	0.612	5.988	0.783	-0.306	10.081	1.283	0.000	14.602	0.956	0.191	24.072	1.084	-0.089
1.955	1.140	0.459	6.049	0.759	-0.382	10.142	1.283	0.000	14.724	0.981	0.210	24.256	1.065	-0.102
2.016	1.166	0.421	6.110	0.736	-0.382	10.203	1.283	0.000	14.847	1.009	0.229	24.439	1.044	-0.115
2.077	1.194	0.459	6.171	0.720	-0.268	10.264	1.283	0.000	14.969	1.033	0.191	24.622	1.026	-0.102
2.138	1.234	0.650	6.232	0.703	-0.268	10.325	1.280	-0.038	15.091	1.051	0.153	24.805	1.005	-0.115
2.200	1.262	0.459	6.293	0.689	-0.229	10.387	1.278	-0.038	15.213	1.072	0.172	24.989	0.986	-0.102
2.261	1.287	0.421	6.354	0.673	-0.268	10.448	1.273	-0.076	15.335	1.089	0.134	25.172	0.965	-0.115
2.322	1.304	0.268	6.415	0.664	-0.153	10.509	1.269	-0.076	15.458	1.107	0.153	25.355	0.949	-0.089
2.383	1.329	0.421	6.476	0.654	-0.153	10.570	1.262	-0.115	15.580	1.124	0.134	25.539	0.935	-0.076
2.444	1.353	0.382	6.537	0.645	-0.153	10.631	1.257	-0.076	15.702	1.138	0.115	25.722	0.925	-0.051
2.505	1.376	0.382	6.599	0.638	-0.115	10.692	1.250	-0.115	15.824	1.147	0.076	25.905	0.916	-0.051
2.566	1.395	0.306	6.660	0.633	-0.076	10.753	1.241	-0.153	15.946	1.159	0.096	26.089	0.904	-0.064
2.627	1.411	0.268	6.721	0.629	-0.076	10.814	1.234	-0.115	16.069	1.168	0.076	26.272	0.895	-0.051
2.688	1.430	0.306	6.782	0.626	-0.038	10.875	1.224	-0.153	16.191	1.173	0.038	26.455	0.893	-0.013
2.749	1.442	0.191	6.843	0.626	0.000	10.936	1.213	-0.191	16.313	1.178	0.038	26.638	0.902	0.051
2.810	1.463	0.344	6.904	0.631	0.076	10.998	1.201	-0.191	16.435	1.185	0.057	26.822	0.916	0.076
2.872	1.477	0.229	6.965	0.633	0.038	11.059	1.185	-0.268	16.557	1.185	0.000	27.005	0.925	0.051
2.933	1.486	0.153	7.026	0.638	0.076	11.120	1.173	-0.191	16.680	1.182	-0.019	27.188	0.939	0.076
2.994	1.491	0.076	7.087	0.647	0.153	11.181	1.159	-0.229	16.802	1.180	-0.019	27.372	0.956	0.089
3.055	1.495	0.076	7.148	0.657	0.153	11.242	1.150	-0.153	16.924	1.180	0.000	27.555	0.972	0.089
3.116	1.502	0.115	7.209	0.671	0.229	11.303	1.140	-0.153	17.046	1.171	-0.076	27.738	0.986	0.076
3.177	1.509	0.115	7.271	0.685	0.229	11.364	1.129	-0.191	17.168	1.161	-0.076	27.921	1.000	0.076
3.238	1.512	0.038	7.332	0.699	0.229	11.425	1.114	-0.229	17.291	1.150	-0.096	28.105	1.012	0.064
3.299	1.516	0.076	7.393	0.713	0.229	11.486	1.103	-0.191	17.413	1.138	-0.096	28.288	1.028	0.089
3.360	1.519	0.038	7.454	0.727	0.229	11.547	1.086	-0.268	17.535	1.121	-0.134	28.471	1.040	0.064
3.421	1.523	0.076	7.515	0.745	0.306	11.608	1.072	-0.229	17.657	1.107	-0.115	28.655	1.051	0.064
3.483	1.528	0.076	7.576	0.762	0.268	11.670	1.056	-0.268	17.779	1.093	-0.115			
3.544	1.535	0.115	7.637	0.778	0.268	11.731	1.042	-0.229	17.902	1.075	-0.153			
3.605	1.542	0.115	7.698	0.799	0.344	11.792	1.028	-0.229	18.024	1.056	-0.153			
3.666	1.542	0.000	7.759	0.820	0.344	11.853	1.014	-0.229	18.146	1.035	-0.172			
3.727	1.537	-0.076	7.820	0.843	0.382	11.914	0.995	-0.306	18.268	1.012	-0.191			
3.788	1.535	-0.038	7.882	0.862	0.306	11.975	0.974	-0.344	18.390	0.986	-0.210			
3.849	1.533	-0.038	7.943	0.881	0.306	12.036	0.960	-0.229	18.512	0.967	-0.153			
3.910	1.521	-0.191	8.004	0.902	0.344	12.097	0.944	-0.268	18.635	0.946	-0.172			
3.971	1.512	-0.153	8.065	0.923	0.344	12.158	0.930	-0.229	18.757	0.930	-0.134			
4.032	1.498	-0.229	8.126	0.942	0.306	12.219	0.918	-0.191	18.879	0.916	-0.115			
4.094	1.491	-0.115	8.187	0.965	0.382	12.281	0.907	-0.191	19.001	0.904	-0.096			
4.155	1.484	-0.115	8.248	0.988	0.382	12.342	0.895	-0.191	19.123	0.888	-0.134			
4.216	1.474	-0.153	8.309	1.007	0.306	12.403	0.879	-0.268	19.246	0.876	-0.096			

developed flows in long tubes, and that the short oscillatory motions of vertical columns are similar to flows in short tubes. In such cases, adjustments of coefficients to the different experimental conditions must always be made (they follow naturally). The periods of oscillation obtained from the experiments using $H_R=7.5$ cm and 5.8 cm were 0.534 s and 0.500 s, respectively, calculated using the first and second peaks of oscillation. The adjusted coefficients allowed obtaining periods of 0.565 s and 0.500 s, very close to the measured values.

Small scale experiments are easily built and more expeditious to furnish results, quickly generating sets of data. The comparison made here show that they may be used for the first tests of numerical models, related to the evolution of the water level, the velocity, and the magnitude of the periods of oscillation. Because small setups involve capillary effects, not considered in the present formulation, deviations between experimental and calculated results may eventually be observed for larger times.

4.3 Results of the Large Setup

Equation (9) with constant coefficients reproduces the usual approach of developed turbulent flows, valid for high Reynolds numbers. Large scale applications are more usual in engineering, like vertical tubes in drainage and water distribution systems, where capillary effects are not relevant.

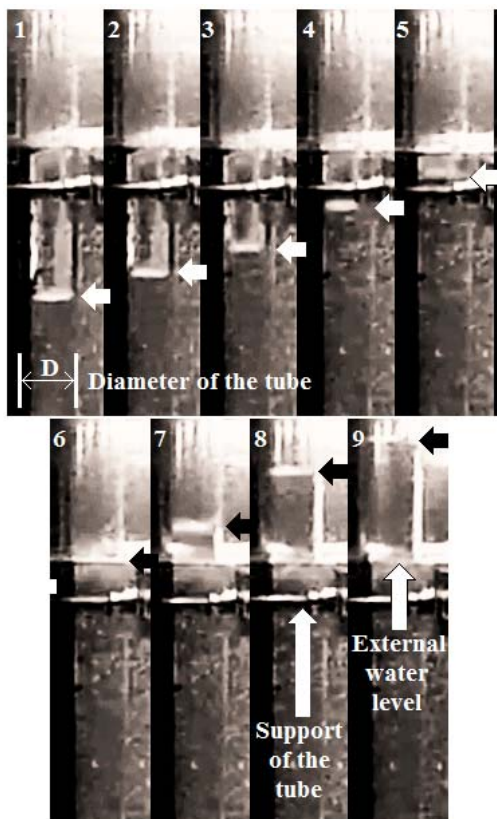


Fig. 8. Snapshots of one of the movies used to measure the level and the velocity of the internal water surface for the large setup.

Figure 8 shows snapshots of one of the movies of the large setup (Fig. 3). Slides 1 to 5 (upper part of the figure) show the internal level of the water while positioned below the external surface level (white horizontal arrows). Slides 6 to 9 show the internal level of the water positioned above the external surface level (black horizontal arrows).

Table 3 was obtained for free oscillations (not damped) in the large setup (diameter of 2.54 cm).

Even for large setups the vertical motion in the tube involves instants of rest, with corresponding low Reynolds numbers for displacements “close to the rest”. But the highest Reynolds number was now 36,400, generating fluctuations and secondary movements (not immediately damped), so that turbulence was more likely present. Adjustments of coefficients and friction factors are thus needed in all scales of work.

Figure 9 shows the normalized velocity against the normalized depth for $D=2.54$ cm and $H_R=18.25$ cm. The normalized immersion length H_R/D was 7.2. Because some “blurring” of the images, regarded to the position of the surface, upper and lower limiting values for this position were marked in each frame. Velocities were calculated for the upper and lower registers, and for their mean value. Table 3 shows the mean depths and corresponding velocities. The graph of Fig. 9 shows the convergence to the fixed point, and that the velocity values oscillate intensively. The measured instantaneous velocity is strongly dependent on the quality of the measurements of the surface positions.

Figure 10 shows the normalized water depths of Table 3 against the normalized time. Simulation and data follow similar trends, with similar periods and amplitude damping (blue dots and continuous line). Like for the smaller diameter ($D=0.62$ cm), also here a shift in the calculated time origin was used. The observed period of oscillation in Table 3 is 0.878 s, obtained as mean value the four height peaks. The calculated numerical value is 0.869 s, also very close to the measured result.

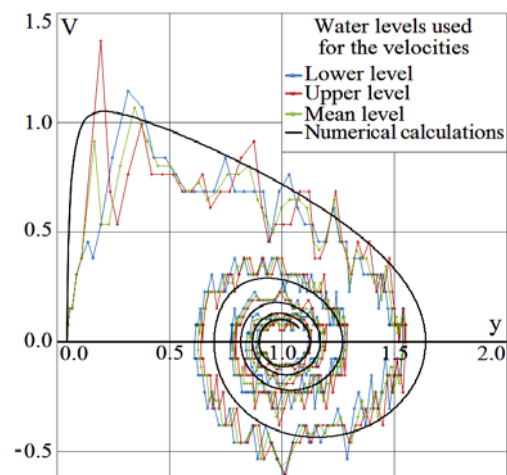


Fig. 9. Experimental data of Table 3 and numerical calculations of Eq. (9) using $\theta_2=0.1$, $\theta_3=0.7$, $\Delta\tau=0.01$.

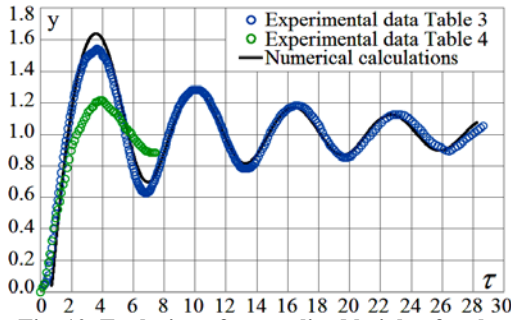


Fig. 10. Evolution of normalized heights for the conditions of Fig. 9 (blue dots and solid line), and damped oscillations of Table 4 (green dots).

4.4 Joint Results

The nondimensional results for the periods of the experiments and of the numerical calculations are close to the value $\tau=6.4$. The maximum difference from the value 2π is only about 3%. The periods of oscillation may thus be calculated with a good degree of approximation, for vertical nonlinear oscillations that follow Eq. (9), by:

$$T = 2\pi \sqrt{\frac{H_R}{g}} \tag{21}$$

This is the period for oscillations in “U tubes”, for which $H_R=L/2$, being L the total length of the oscillating volume of water. The experimental data for $D=0.62$ cm were followed by the numerical results by using $\theta_2=0.3$ and $\theta_3=1.0$, while for $D=2.54$ cm the coefficients were adjusted to $\theta_2=0.1$ and $\theta_3=0.7$. The agreement observed in Figs. 6, 7, 9 and 10 also show that the coefficients θ_2 and θ_3 depend on the scale of the experiment. For the data of this study it was necessary to use lower values of the coefficients for larger diameters of the tube.

The motion observed in small diameters, subjected to capillary effects, has shown similar behavior to that occurring in larger diameters when using nondimensional variables and taking the periods as function of the length H_R (expressed by Eq. 21).

Considering the good adherence of the results to Eq. (21), a run imposing oscillation damping at the air phase was also performed, intending to verify eventual adherence to this equation. The water in the tube with $D=2.54$ cm and H_R adjusted to 18.25 cm was induced to oscillate while capped as shown in Fig. 3a. The device consisted of an impermeable cap having an opening with diameter of 0.48 cm, to which a hose with the same diameter and length of 30 cm was attached, followed by a straight tube with diameter of 0.70 cm and length of 21.5 cm. This arrangement imposed a head loss in the flow of the gaseous phase that strongly reduced the amplitude of the movement. But the measured period of oscillation presented the value of 0.908 s, thus close to the previous value of 0.878 s. The difference is only of about 3.4%, and it may still be related to eventual differences in the value of H_R . Fig. 10 shows the first period of oscillation of this damped experiment, which values are furnished in

Table 4. Eq. (21) may thus be used as approximation even for damping of oscillations occurring in the air phase using orifices and hoses like described here.

Table 4 Data for $D=2.54$ cm, 60 fps.

H_R (cm)=18.25			
t s	h cm	t s	h cm
0.000	0.00	0.517	22.18
0.017	0.55	0.533	22.18
0.033	1.01	0.550	22.18
0.050	2.24	0.567	21.93
0.067	3.37	0.583	21.72
0.083	4.39	0.600	21.35
0.100	5.98	0.617	21.13
0.117	7.42	0.633	20.92
0.133	8.56	0.650	20.86
0.150	9.57	0.667	20.67
0.167	10.52	0.683	20.37
0.183	11.47	0.700	20.09
0.200	12.42	0.717	19.57
0.217	13.13	0.733	19.29
0.233	14.35	0.750	18.96
0.250	15.40	0.767	18.80
0.267	16.35	0.783	18.56
0.283	17.08	0.800	18.34
0.300	17.51	0.817	17.94
0.317	18.22	0.833	17.64
0.333	18.71	0.850	17.45
0.350	18.96	0.867	17.12
0.367	19.45	0.883	16.90
0.383	19.91	0.900	16.69
0.400	20.34	0.917	16.47
0.417	20.83	0.933	16.32
0.433	21.04	0.950	16.26
0.450	21.35	0.967	16.13
0.467	21.44	0.983	16.13
0.483	21.93	1.000	16.13
0.500	22.02	1.017	16.13

Upwards and downwards motions were calculated using the same values of θ_2 and θ_3 , not showing relevant deviations from the observed data in the oscillation periods reproduced here.

The theoretical solution was obtained for integer values of $N=2\theta_3$. The adjustment of the calculations to the experimental data showed that θ_3 may have fractional character, for which the differential Eq. (9) was solved numerically.

4.5 Water Ejection

As mentioned in the introduction, vertical tubes in distribution or drainage systems may be subjected to geyser events. When subjected to internal water oscillations, vertical tubes may produce ‘momentary geysers’, or water ejections, due to the upwards acceleration of the water column. It is evident in Fig. 7 that if the vertical pipe is shorter than ~ 1.40 (that is, about 0.40 above the equilibrium level $y=1.0$) the ascending water spills out of the pipe, that is, the amplitude of the movement is larger than the remaining pipe length. The velocity of ejection depends on the length of the tube and its diameter, combined factors that may inhibit the acceleration of the column. Fig. 11 shows a water ejection for the tube of $D=0.62$ cm and $H_R=15.3$ cm. The upper cross section of the tube (position indicated as L in the figure) was maintained 0.25 cm above the water surface. The water was spilled until a height of $2.2 D$ from the upper end of the tube.

All the experiments of this study were performed by applying an initial displacement with value close to H_R , below the water surface of the reservoir, thus implying in ascending initial movement.

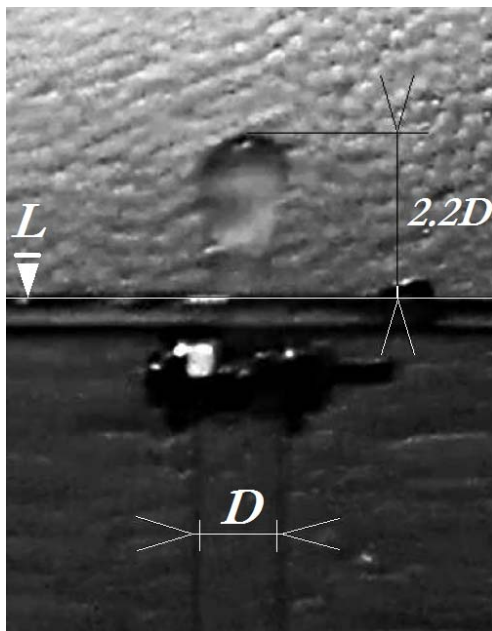


Fig. 11. Vertical water ejection, for $D=0.62$ cm, $H_R=15.3$ cm. L indicates the level of the upper cross section of the vertical tube.

5. CONCLUSION

Oscillations of water in vertical tubes, directed to the studies of water distribution systems, drainage systems, and oscillation suppressing devices, were subjected to theoretical and experimental analyses.

For the theoretical analysis a nonlinear second order governing equation for the motion was presented, with two coefficients involving local and distributed energy losses. Both coefficients were multiplied by the square of the velocity. This condition reflects

fully developed turbulent flows when using constant coefficients. Its solution is composed by a set of two equations, one for the upwards and other for the downwards motions, which depend on the two mentioned coefficients for the energy losses in the flow, and which lead to a cyclic behavior when used together. Theoretical solution and numerical calculations showed very good agreement.

For the experimental analyses, results were obtained in adequately prepared semi-immersed tubes using diameters of 0.62 cm and 2.54 cm, and different immersion lengths. The behaviors of the observed water level and the velocity were well reproduced by the calculations.

Data of free oscillations were obtained for both the small and the large setups. Data for damped oscillations were generated using the large setup by imposing energy losses for the air that moves due the water oscillations. The experimental results show that the periods of oscillation for all tested conditions are approximated by Eq. (21), suggesting further studies to check the observed tendency.

Finally, it was shown that water may spill out of the vertical tube above the level of the reservoir, as momentary water ejections, depending on the geometry of the tube and the oscillation amplitude.

A very good agreement between experimental, analytical and numerical results was observed, suggesting further studies for engineering purposes.

ACKNOWLEDGEMENTS

The first author thanks CAPES, Brazil, for the grant BEX 5723/15-9, and the University of Alberta, Canada, for the research period of 2016/2017.

REFERENCES

- Benattalah, S., F. Aloui and M. Souhar (2011). Experimental Analysis on the Counter-Current Dumitrescu-Taylor Bubble Flow in a Smooth Vertical Conduct of Small Diameter, *Journal of Applied Fluid Mechanics* 4(4), 1-14.
- Churchill, S. W. (1977). Friction factor equations spans all fluid-flow regimes, *Chem. Eng.* 84(24), 91-92.
- El-Behery, S. M., A. A. El Haroun and M. R. Abuhegazy (2017). Prediction of Pressure Drop in Vertical Pneumatic Conveyors, *Journal of Applied Fluid Mechanics*, 10(2), 519-527.
- Lorenceanu, E., D. Quéré, J. Y. Ollitrault and C. Clanet (2002). Gravitational oscillations of a liquid column in a pipe, *Physics of Fluids* 14 (6), 1985-1992.
- Lou, S., G. H. Zhong, Y. D. Zhu and S. G. Liu (2008). Investigation of Underground Traffic Facilities for Flood Control in Shanghai. *Proc. of the 5th China-Japan Joint Seminar for the Graduate Students in Civil Engg.*, Tongji University, Shanghai, China 136-141.

- Masoodi, R.; E. Languri and A. Ostadossein (2013). Dynamics of liquid rise in a vertical capillary tube, *J. of Colloid and Interfacial Science* 389, 268-272.
- Politano, M., J. Odgaard and W. Klecan (2005). Numerical Simulation of Hydraulic Transients in Drainage Systems. *Mecánica Computacional*, XXIV, 297-310.
- Quéré, D. and É. Raphaël (1999). Rebounds in a capillary tube, *Langmuir* 15(10), 3679–3682.
- Weidman, P. and I. Kliakhandler (2014). Gravitational oscillations of a capped liquid-air column, *Physics of Fluids*, 26(4).
- Weidman, P. D., B. Roberts and S. Eisen (2012). On the Instability of Spheres Settling through a Vertical Pipe Filled with HPG, *Journal of Applied Fluid Mechanics* 5(4), 113-121.
- Zhmud, B.V., K. Tiberg and J. Hallstensson (2000) Dynamics of Capillary Rise, *J. of Colloid and Interface Science* 228, 263– 269